Second-Harmonic Generation Measurements of Electrostatic Biopolymer−Surfactant Coadsorption at the Water/1,2-Dichloroethane Interface

Hillary J. Paul and Robert M. Corn*

Department of Chemistry, University of Wisconsin—Madison, 1101 University Avenue, Madison, Wisconsin 53706

Received: February 28, 1997; In Final Form: April 15, 1997[⊗]

The electrostatic coadsorption of the synthetic polypeptide poly-L-glutamic acid (pGlu) and the cationic hemicyanine surfactant *trans*-4-[4-(dibutylamino)styryl]-1-methylpyridinium iodide (D^+-CH_3) is observed at the water/1,2-dichloroethane (DCE) interface with the spectroscopic technique of optical second-harmonic generation (SHG). The adsorption isotherm of D^+-CH_3 to the water/DCE interface is obtained with a combination of resonant surface SHG and interfacial tension measurements. In the presence of polyanionic pGlu in the aqueous phase at a pH of 8.5, the limiting surface coverage of the cationic surfactant is enhanced by a factor of 3.7. In contrast, no such enhancement is observed in the presence of pGlu for the adsorption of the neutral zwitterionic hemicyanine surfactant *trans*-4-[4-(dibutylamino)styryl]-1-(3-sulfopropyl)pyridinium hydroxide inner salt hydrate ($D^+-(CH_2)_3-SO_3^-$) to the water/DCE interface. Additionally, no enhancement in surfactant adsorption is observed for D^+-CH_3 when the pGlu in the aqueous phase is replaced with a solution of the monomer L-glutamic acid. These observations demonstrate that the coadsorption of pGlu and D^+-CH_3 is a multipoint electrostatic adsorption interaction at the water/DCE interface.

Introduction

The nonspecific electrostatic adsorption of proteins and polypeptides onto charged surfaces occurs frequently in biological membrane systems[1−3] and also serves as the basis for a variety of bioanalytical sensor devices and affinity chromatography schemes at metal and oxide surfaces.[4−7] For example, charged self-assembled monolayers have recently been used to create electrostatically adsorbed polypeptide monolayers [8−10] and even multilayers.[11−13] At the water/1,2-dichloroethane (DCE) interface, the adsorption of surfactants and phospholipids has been shown to create a variety of charged monolayers at the interface.[14−22] If the surfactant contains a nonlinear optical chromophore, this monolayer formation can be followed with the spectroscopic technique of optical second-harmonic generation (SHG).[19,18,23] In this paper, we use resonant surface SHG measurements to demonstrate that multiply charged polypeptides can be coadsorbed with a charged surfactant at the water/DCE interface by an electrostatic adsorption mechanism. The presence of the biopolymer at the interface results in an enhanced surfactant adsorption that is monitored with the SHG measurements. A schematic representation of the electrostatic biopolymer−surfactant coadsorption process is shown in Figure 1.

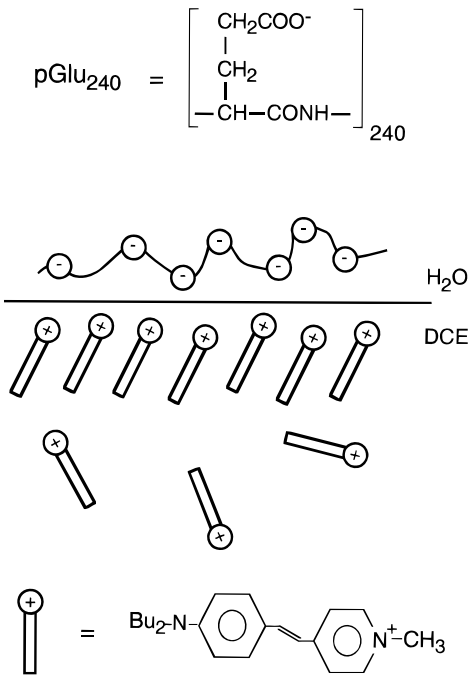

Figure 1. Schematic diagram of the biopolymer−surfactant coadsorption process. In the presence of the synthetic polypeptide, poly-L-glutamic acid, a multipoint electrostatic coadsorption process occurs, resulting in an increased surface coverage of the cationic surfactant, D^+-CH_3.

Results and Discussion

The formation of the coadsorbed surfactant−biopolymer monolayer at the water/DCE interface is followed by monitoring the surface coverage of the surfactant molecules with resonant SHG measurements. Resonant SHG has been used frequently to monitor the adsorption, orientation, and organization of molecules at liquid/liquid, liquid/solid, and liquid/air surfaces.[24−26] The surface specificity of this nonlinear optical technique makes it an ideal choice for studying adsorption of monolayers of soluble surfactant molecules that are in equilibrium with the bulk phase(s). For these experiments, two soluble surfactant molecules that contain an SHG-active hemicyanine nonlinear chromophore are employed: *trans*-4-[4-(dibutylamino)styryl]-1-methylpyridinium iodide (D^+-CH_3) and *trans*-4-[4-(dibutylamino)styryl]-1-(3-sulfopropyl)pyridinium hydroxide inner salt hydrate ($D^+-(CH_2)_3-SO_3^-$). These two molecules have UV−visible absorption maxima in DCE at 534 and 516 nm, respectively; SHG measurements that employ a fundamental wavelength of 1064 nm are greatly enhanced by a resonance with these molecules at the second-harmonic wavelength.[24,27] To further increase the SHG from the water/DCE interface, a total internal reflection (TIR) geometry is employed.[20,28,29] Since the molecules are soluble in both water and DCE, small self-

[⊗] Abstract published in *Advance ACS Abstracts,* May 15, 1997.

S1089-5647(97)00751-7 CCC: $14.00

absorption corrections were made at the highest surfactant concentrations (above 1 μM). A small nonresonant background from the water/DCE interface corresponding to less than 0.4% of a full monolayer was observed.

In this paper, the resonant molecular surface SHG signal from the adsorbed surfactant monolayer is used to monitor the surface coverage of the adsorbed molecules. In addition to surface coverage measurements, it is also possible to determine the average molecular orientation of the adsorbed species by measuring the polarization dependence of the SHG signal.[30,31,25] For the surfactant molecules D^+-CH_3 and $D^+-(CH_2)_3-SO_3^-$ at the water/DCE interface, the molecular orientation parameter[19] D for both molecules is roughly 0.53, as obtained from a series of SHG polarization measurements. This orientation parameter corresponds to an average orientation angle of 43° with respect to the surface normal. The orientation angle for both molecules did not change as a function of surface coverage, so that the changes in the SHG intensity can be directly related to the changes in surface coverage. In particular, as in previous studies,[19,23] the square root of the SHG intensity was used to monitor the relative surface coverage of the adsorbate, θ, where θ is equal to Γ/Γ_{max}, and Γ_{max} is the maximum surface coverage for the species.

In order to relate the SHG signal to an absolute surface coverage, the maximum surface coverage, Γ_{max}, was obtained by interfacial tension measurements using the Wilhelmy plate method.[32,18] From the limiting slope of a plot of the interfacial tension versus ln(C), where C is the concentration of the surfactant molecule in the bulk, we were able to estimate Γ_{max} of each surfactant system. For D^+-CH_3 at the water/DCE interface, Γ_{max} is approximately 2.7×10^{13} molecules/cm^2, while for $D^+-(CH_2)_3-SO_3^-$ it is slightly larger at 5.0×10^{13} molecules/cm^2. Once Γ_{max} is known for each surfactant system, the relative surface coverage, θ, obtained in the SHG experiments can be converted to an absolute surface coverage (molecules/cm^2) Γ by the relationship given above.

The adsorption isotherms for each of the two surfactants, as obtained from a combination of SHG and interfacial tension measurements, are shown in Figure 2. Surface coverages as low as 3% of a full monolayer were measured in the TIR geometry for these surfactants. At these low surface coverages, the interactions between adsorbed species is less significant, and the adsorption isotherm was found to be linear. This region of the isotherm can be described by a simple Langmuir expression: $\Gamma \approx \Gamma_{max}\beta C$. The Langmuir adsorption coefficient, β, is found at low surface coverage from the slope of Γ versus C and the value for Γ_{max}, as determined by the interfacial tension measurements. For the cation and the zwitterion, β is found to be 1.8×10^5 and 3.6×10^5 M^{-1}, respectively. The full isotherms shown in Figure 2 follow Frumkin adsorption behavior, indicating that there is some interaction between the adsorbed species as a function of surface coverage. The Frumkin adsorption isotherm is described by the following expression:[33]

$$\beta C = \frac{\theta}{1-\theta}\exp(g\theta) \qquad (1)$$

In this equation, C is the concentration of the surfactant in the bulk, β is the Langmuir adsorption coefficient, θ is the relative surface coverage (Γ/Γ_{max}), and g is the Frumkin interaction parameter. Using β and Γ_{max} found above for each surfactant system, the Frumkin interaction parameter, g, was obtained by fitting eq 1 to the data in Figure 2. The value of g for both the cation and the zwitterion is negative (−1.2 and −1.8, respectively), indicating that the interaction between adsorbed species is repulsive. A second indication that repulsive interactions are important in these monolayers is obtained by converting Γ_{max} to an average area per molecule. For comparison, a typical value for the average area per molecule for a similar hemicyanine surfactant that has been compressed by a Langmuir−Blodgett technique at the air−water interface is approximately 20 Å^2/molecule.[34] The cation and the zwitterion have an area per molecule of 370 and 200 Å^2/molecule, respectively. This larger area per molecule indicates that there are repulsive interactions preventing the adsorbed species from packing more tightly at the interface.

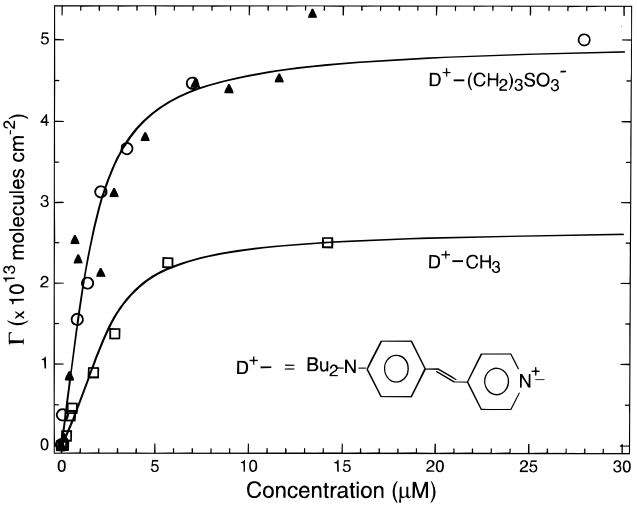

Figure 2. Concentration isotherms for the cationic surfactant, D^+-CH_3, and the neutral zwitterionic surfactant, $D^+-(CH_2)_3-SO_3^-$ at the water/DCE interface. The open squares represent the SHG data for the cationic species, while SHG and interfacial tension data for the zwitterionic species are represented by open circles and triangles, respectively. The resonant SHG data for each surfactant was converted from relative surface coverage to absolute surface coverage by the relationship $\Gamma = \Gamma_{max}\theta$. Γ_{max} was determined by interfacial tension measurements for each surfactant. In the absence of supporting electrolyte, Γ_{max} is higher for the zwitterionic surfactant than for the cationic surfactant. The solid lines are Frumkin fits to the SHG data.

A second set of SHG measurements, shown in Figure 3, demonstrates that the maximum surface coverage of the cationic surfactant, D^+-CH_3, at the water/DCE interface is enhanced when $pGlu_{240}$ is added to the aqueous phase. Interfacial tension measurements indicate that $pGlu_{240}$ does not adsorb to the water/DCE interface in the absence of the cationic surfactant. The isotherms for D^+-CH_3 with and without $pGlu_{240}$ in Figure 3 show an increase by nearly a factor of 4 in the D^+-CH_3 surface coverage upon addition of $pGlu_{240}$ at a pH of 8.5. In these experiments, the SHG signal was determined in the following manner: For each solution of varying concentration of D^+-CH_3 in DCE, an aliquot of $pGlu_{240}$ was injected into the sample cell in the aqueous phase. The final concentration of $pGlu_{240}$ in the aqueous phase was 2.8 μg/mL, corresponding to 18 μM in glutamate residues. The SHG signal in the presence of $pGlu_{240}$ was recorded 90 min after the $pGlu_{240}$ injection. As in the previous experiments, the orientation angle of the surfactant molecules did not change upon addition of $pGlu_{240}$, and the square root of the SHG signal was directly related to the relative surface coverage of D^+-CH_3. The maximum surface coverage at this interface in the absence of the $pGlu_{240}$ is roughly 1.0×10^{14} molecules/cm^2 and in the presence of $pGlu_{240}$ is estimated to be approximately 3.6×10^{14} molecules/cm^2. Surface tension measurements confirm Γ_{max} for D^+-CH_3 in the presence of $pGlu_{240}$. The above values for Γ_{max} correspond to a decrease in the average area per molecule from nearly 100 to 30 Å^2/molecule.

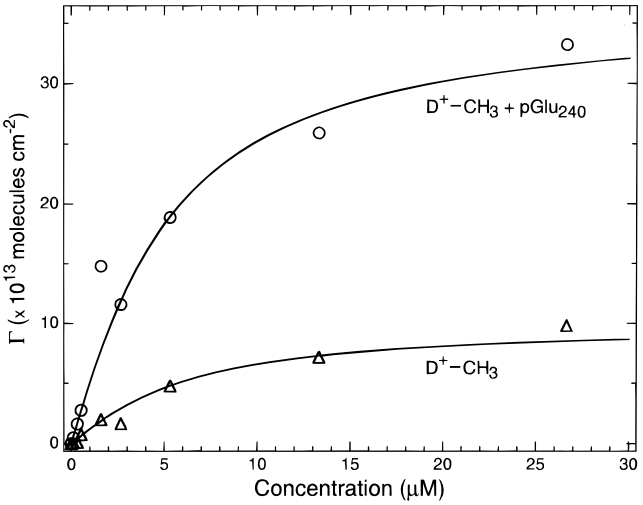

Figure 3. Concentration isotherms for D^+-CH_3 in the presence (open circles) and absence (open triangles) of $pGlu_{240}$ as obtained by SHG measurements. The absolute surface coverage shown above was determined from the relative surface coverage, obtained from the SHG data, and Γ_{max} estimated by interfacial tension measurements. The $pGlu_{240}$ was added to the aqueous phase at a pH of 8.5, buffered with 10 mM $NaHCO_3$. The final $pGlu_{240}$ concentration in the aqueous phase was 2.8 μg/mL, corresponding to a residue concentration of 18 μM. In the presence of 10 mM $NaHCO_3$ buffer, the maximum surface coverage of D^+-CH_3 is about a factor of 4 larger than in the absence of electrolyte as shown in Figure 2. Furthermore, the limiting surface coverage of D^+-CH_3 increased by nearly another factor of 4 in the presence of the $pGlu_{240}$. The solid lines are Frumkin fits to the SHG data.

Note that the maximum surface coverage in the absence of the $pGlu_{240}$ shown in Figure 3 is larger than the maximum surface coverage for the cation shown in Figure 2. This difference arises because a 10 mM $NaHCO_3$ buffer solution was used as the aqueous phase for all data shown in Figure 3, and there was no added electrolyte for data presented in Figure 2. The observed increase in surfactant adsorption is attributed to the partial screening of the head groups on the D^+-CH_3 species by the electrolyte. Both isotherms again demonstrate Frumkin adsorption behavior, and the interaction parameters are again negative (-0.6 for both surfactants). The magnitude of the interaction parameter is smaller than for the isotherms shown in Figure 2; this suggests that the interaction between the adsorbed species is less important in the presence of electrolyte. The Langmuir adsorption coefficients, determined at low surface coverages, were found to be 1.5×10^5 and 1.3×10^5 M^{-1} with and without $pGlu_{240}$, respectively.

In order to test the hypothesis of an electrostatic surfactant−biopolymer coadsorption process, a series of time course experiments were run in order to observe the signal evolution as the polyanion was added to the aqueous phase for several surfactant systems. If the increase in D^+-CH_3 adsorption upon addition of $pGlu_{240}$ is the result of electrostatic interactions, then if the cation is replaced by an uncharged surfactant we would expect to see no enhancement in the signal upon addition of the polyanion. A set of data that plots the square root of the SHG versus time for both the charged and neutral surfactants is shown in Figure 4a. It can be seen that the surface coverage of the cation (circles) increased when the $pGlu_{240}$ was injected by a factor of approximately 3.7 ± 0.3. The transport of the $pGlu_{240}$ to the interface is dependent upon both convection and diffusion, so that the signal does not immediately begin to rise upon injection of $pGlu_{240}$. Once the polyanion reaches the interface, an additional time dependence was observed that is attributed to a combination of adsorption kinetics and to additional diffusion and convection effects. In a second experiment, also shown in Figure 4a, the cation was replaced by the neutral surfactant $D^+-(CH_2)_3-SO_3^-$. After addition of $pGlu_{240}$, no increase in the adsorption of $D^+-(CH_2)_3-SO_3^-$ was observed. These results confirm the hypothesis that the surfactant−biopolymer coadsorption process is an electrostatic interaction.

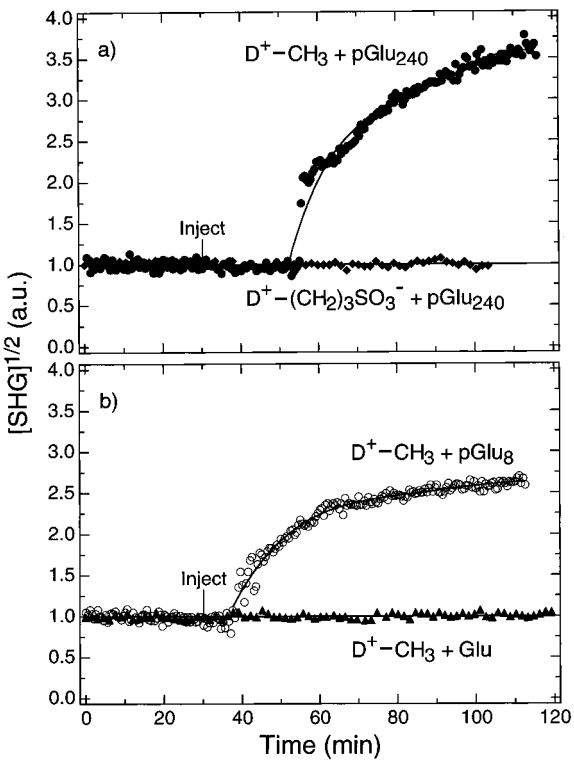

Figure 4. Series of time course experiments showing the signal evolution as (a) $pGlu_{240}$ is injected into samples containing D^+-CH_3 (filled circles) or $D^+-(CH_2)_3-SO_3^-$ (filled diamonds) adsorbed at the water/DCE interface and as (b) $pGlu_8$ (open circles) or Glu (filled triangles) is injected into a sample containing D^+-CH_3 adsorbed at the water/DCE interface. In this set of experiments, it is shown that in order for the coadsorption process to occur, a multipoint electrostatic interaction between the surfactant and the biopolymer must exist. The final concentration of the glutamate residues in each run was 25 μM in the aqueous phase. The concentration of the surfactant in the bulk DCE was 2 μM. Note that the solid lines are shown only to guide the eye.

In Figure 4b, a second set of time dependent data is shown for the adsorption of D^+-CH_3 following the addition of the monomer L-glutamic acid and $pGlu_8$. The circles and solid curve represent the signal evolution after adding $pGlu_8$ to the aqueous phase. In this case, the cation surface coverage increased by a factor of approximately 2.7 ± 0.1. A comparison of parts a and b of Figure 4 clearly shows that the larger polymer gives rise to an increased adsorption of the cationic species as compared to the shorter polymer. Furthermore, the maximum signal reached equilibrium more quickly for $pGlu_8$. This effect is most likely the result of faster diffusion to the interface and surface reorganization for the lower molecular weight polymer. When the monomer L-glutamic acid was added to the aqueous phase instead of $pGlu_8$, no increase in SHG from the D^+-CH_3 monolayer was observed. This result suggests that not only is the coadsorption interaction an electrostatic process but that this process is also a multipoint interaction of the pGlu with the surfactant monolayer.

In summary, the resonant SHG measurements in this Letter demonstrate unequivocally that a multipoint electrostatic coadsorption process leads to the formation of an adsorbed bilayer

of the synthetic polypeptide poly-L-glutamic acid with the cationic surfactant D^+-CH_3 at the water/DCE interface. The formation of the bilayer at the interface enhances the adsorption of D^+-CH_3, with the limiting surface coverage increasing by a factor of 3.7 upon addition of $pGlu_{240}$ and by a factor of 2.7 for $pGlu_8$. The coadsorption process described in this Letter is expected to be universal for a variety of biopolymer−surfactant systems. In preliminary work we have observed a similar interaction between poly-L-lysine and stearic acid at the water/DCE interface via interfacial tension measurements. Also, it should be possible to enhance or destroy the bilayer formation by controlling an applied potential across the liquid/liquid interface. In future research, we will tag the biopolymer with a nonlinear optical probe and monitor the adsorption of the polypeptide directly with resonant SHG. A second possibility will be to monitor the biopolymer adsorption process with other techniques, such as circular dichroism SHG[35−38] or optical rotary dispersion SHG.[39]

Acknowledgment. The authors gratefully acknowledge the National Science Foundation for support of this research.

References and Notes

(1) Dryhurst, G.; Kadish, K. M.; Scheller, F.; Renneberg, R. *Biological Electrochemistry*; Academic Press: New York, 1982.
(2) Roth, C. M.; Lenhoff, A. M. *Langmuir* **1995**, *11*, 3500.
(3) Elgersma, A. V.; Zsom, R. L.; Norde, W.; Lyklema, J. *J. Colloid Interface Sci.* **1990**, *138*, 145.
(4) Cass, A. E. G., Ed. *Biosensors, A Practical Approach*; Oxford University Press: New York, 1990.
(5) Decher, G.; Lehr, B.; Lowack, K.; Lvov, Y.; Schmitt, J. *Biosens. Bioelectron.* **1994**, *9*, 677.
(6) Turner, A. P. F., Karube, I., Wilson, G. S., Eds. *Biosensors: Fundamentals and Applications*; Oxford University Press: Oxford, 1987.
(7) Smith, M. C.; Furman, T. C.; Pidgeon, C. *Inorg. Chem.* **1987**, *26*, 1965.
(8) Blaakmeer, J.; Cohen-Stuart, M. A.; Fleer, G. J. *J. Colloid Interface Sci.* **1990**, *140*, 314.
(9) Jordan, C. E.; Corn, R. M. *Anal. Chem.* **1997**, *69*, 1449.
(10) Jordan, C. E.; Frey, B. L.; Kornguth, S.; Corn, R. M. *Langmuir* **1994**, *10*, 3642.
(11) Lvov, Y.; Decher, G.; Sukhorukov, G. *Macromolecules* **1993**, *26*, 5396.
(12) Lvov, Y.; Ariga, K.; Ichinose, I.; Kunitake, T. *J. Am. Chem. Soc.* **1995**, *117*, 6117.
(13) Cooper, T. M.; Campbell, A. L.; Crane, R. M. *Langmuir* **1995**, *11*, 2713.
(14) Girault, H. J.; Schiffrin, J. *J. Electroanal. Chem.* **1984**, *179*, 277.
(15) Wandlowski, T.; Marecek, V.; Samec, Z. *J. Electroanal. Chem.* **1988**, *242*, 277.
(16) Cheng, Y.; Schiffrin, D. J. *J. Chem. Soc., Faraday Trans.* **1994**, *90*, 2517.
(17) Kakiuchi, T.; Nakanishi, M.; Senda, M. *Bull. Chem. Soc. Jpn.* **1988**, *61*, 1845.
(18) Higgins, D. A.; Corn, R. M. *J. Phys. Chem.* **1993**, *97*, 489.
(19) Naujok, R. R.; Higgins, D. A.; Hanken, D. G.; Corn, R. M. *J. Chem. Soc., Faraday Trans.* **1995**, *91*, 1411.
(20) Conboy, J. C.; Richmond, G. L. *Electrochim. Acta* **1995**, *40*, 2881.
(21) Vanysek, P. *Electrochemistry on Liquid/Liquid Interfaces*; Springer-Verlag: Berlin, 1985.
(22) Benjamin, I. *Chem. Rev.* **1996**, *96*, 1449.
(23) Naujok, R. R.; Paul, H. J.; Corn, R. M. *J. Phys. Chem.* **1996**, *100*, 10498.
(24) Higgins, D. A.; Corn, R. M. *Chem. Rev.* **1994**, *94*, 107.
(25) Eisenthal, K. B. *Annu. Rev. Phys. Chem.* **1992**, *43*, 627.
(26) Shen, Y. R. *Nature* **1989**, *337*, 519.
(27) Heinz, T. F.; Chen, C. K.; Ricard, D.; Shen, Y. R. *Phys. Rev. Lett.* **1982**, *48*, 478.
(28) Conboy, J. C.; Daschbach, J. L.; Richmond, G. L. *J. Phys. Chem.* **1994**, *98*, 9688.
(29) Bloembergen, N.; Simon, H. J.; Lee, C. H. *Phys. Rev.* **1969**, *181*, 1261.
(30) Heinz, T. F. In *Nonlinear Surface Electromagnetic Phenomena*; Ponath, H. E., Stegeman, G. I., Eds.; North-Holland: Amsterdam, 1991; p 353.
(31) Higgins, D. A.; Corn, R. M. In *Characterization of Organic Thin Films*; Ulman, A., Ed.; Butterworth-Heinemann: Newton, MA, 1995; p 227.
(32) Nakanaga, T.; Takenaka, T. *J. Phys. Chem.* **1977**, *81*, 645.
(33) Bard, A. J.; Faulkner, L. R. *Electrochemical Methods: Fundamentals and Application*; John Wiley & Sons, Inc.: New York, 1980.
(34) Stroeve, P.; Srinivasan, M. P.; Higgins, B.; Kowel, S. *Thin Solid Films* **1987**, *146*, 209.
(35) Byers, J. D.; Yee, H. I.; Petralli-Mallow, T.; Hicks, J. M. *Phys. Rev. B* **1994**, *49*, 14 643.
(36) Petralli-Mallow, T.; Wong, T. M.; Byers, J. D.; Yee, H. I.; Hicks, J. M. *J. Phys. Chem.* **1993**, *97*, 1383.
(37) Verbiest, T.; Kauranen, M.; Persoons, A.; Ikonen, M.; Kurkela, J.; Lemmetyinen, H. *J. Am. Chem. Soc.* **1994**, *116*, 9203.
(38) Hicks, J. M.; Petralli-Mallow, T.; Byers, J. D. *Faraday Discuss.* **1994**, *99*, 341.
(39) Byers, J. D.; Yee, H. I.; Hicks, J. M. *J. Chem. Phys.* **1994**, *101*, 6233.